



Osseointegration of titanium implants modulated by vitamin K₂ and yerba mate extract in an animal model

R. G. Fathi, G. A. Taqa

University of Mosul, Mosul, Iraq

Article info

Received 02.12.2024

Received in revised form

05.01.2025

Accepted 10.02.2025

Department
of Basic Science,
College of Dentistry,
University of Mosul,
Mosul, Iraq.
Tel.: +964-777-399-94-
55. E-mail:
ruaa.22dep2@student.
uomosul.edu.iq

Fathi, R. G., & Taqa, G. A. (2025). Osseointegration of titanium implants modulated by vitamin K₂ and yerba mate extract in an animal model. *Regulatory Mechanisms in Biosystems*, 16(1), e25034. doi:10.15421/0225034

Bone defects are difficult to treat and represent challenges in clinical settings, including dental defects. This study aimed to evaluate the positive osseointegration impact of surface treatment of titanium implants by vitamin K₂ (VK2) and yerba mate (*Ilex paraguariensis* A.St.-Hil.; Aquifoliales, Aquifoliaceae) extract (YME). To do so, we used 18 rabbits with day 1 inserted dental implants in their tibial bone. These 18 rabbits were subdivided into 3 groups; the control group received normal saline, the VK2 group received VK2, and the YME group received YME. For each group, three rabbits were sacrificed on day 30 of the experiment and the remaining three rabbits were sacrificed on day 45 following continuous interventional therapy. Implant insertion was confirmed by radiological analysis and osseointegration was confirmed by histological, proteomic, and genetic analysis. VK2 and YME have been associated with the production of tiny capillaries and collagen-rich membrane structures. The early ossification zones, which were rich in living osteoprogenitor cells and extremely dense in collagen fibre groups, were visible. YME and VK2 led to a nearly one-fold decline in bone MDA (nmol/L) levels in both experimental groups of animals compared to the control group (20.5 ± 0.6). VK2 or YME treatment showed up to a 20–40% rise in bone GSH-Px levels in contrast to the control group (25.8 ± 1.3). In comparison to the control group (20.1 ± 2.1), the treated groups (VK2 and YME) showed significantly higher TAS levels. The bone Runx2 fold change jumped considerably in all treated groups (VK2 and YME) in comparison to the control group (41.6 ± 2.1). The bone osteocalcin fold change jumped considerably in all treated groups (VK2 and YME) in contrast to the control group (11.7 ± 1.3). VK2 and YME facilitated osseointegration and improved bone regeneration together with reduced oxidative stress.

Keywords: yerba mate extract; *Ilex paraguariensis*; dental implant; bone.

Introduction

Natural teeth are commonly lost due to oral diseases such as tooth decay, periodontal diseases, and trauma that affect appearance, speech, and the masticatory system. Aiming to improve patients' quality of life by restoring lost teeth, function, and esthetics, dental implants are commonly used. The use of dental implants based on titanium and titanium alloys is considered to be one of the main treatment options for replacing lost or missing teeth. Such implants are biocompatible, corrosion-resistant, and have favourable mechanical properties. Various surface modifications for titanium dental implants such as blasting, or chemical treatments such as an alkaline treatment, have been used to accelerate and improve the bone healing process. The living bone could become so fused with the titanium oxide layer of the implant that the two could not be separated without fracture. Thus, Brånemark introduced the term osseointegration to describe this modality for stable fixation between titanium and bone tissue. Osseointegration consists of a series of bone modelling and remodelling processes. It has been defined as the direct structural and functional connection between living bone and the surface of a load-bearing artificial implant.

Bone tissue repair mechanisms and bone metabolism are strongly influenced by nutritional aspects and are crucial to obtaining proper bone restoration and optimizing osseointegration processes. Several micronutrients affecting bone metabolism were demonstrated to have an influence on the skeletal system; in particular, calcium, fluorides, magnesium, potassium, vitamin B₆, vitamin D, and zinc positively influence bone health, reducing the risk of fracture. In addition, fat-, carbohydrate-, and cholesterol-rich diets and reduced calcium intake exhibit detrimental influences on jaw bone and alveolar bone. Therefore, a specific diet regimen and micronutrients might play a key role in the different phases of dental implant osseointegration. A general issue concerning VK supplementation studies is the wide range of doses that were administered, the frequent combination with other micronutrients, anti-osteoporotic drugs and the highly variable study duration. The present study aimed to evaluate the systemic effect of

VK2 and YME in promoting osseointegration around titanium dental implants in rabbits confirmed by measuring oxidative markers and bone-forming biomarkers alongside histological and radiological findings.

Material and methods

Study settings. The study is registered in the College of Dentistry, University of Mosul (Ref 1903 on 05.03.2023). The study was conducted in the animal house of the College of Veterinary Medicine, University of Mosul (Mosul, Iraq), over a period of 10/9/2023 to 10/1/2024 with the support and assistance of the College of Dentistry, University of Mosul (Mosul, Iraq).

Animals and housing. A total of eighteen healthy albino rabbits (5–6 months, 1800–2000 g average body weight) were purchased from local markets and were used in this experiment. The animals were housed in metallic cages and subjected to an adaptation period of two weeks with a photoperiod of (12hr: 12hr light/dark), 25 ± 2 °C temperature, and 45–50% humidity while receiving the normal amount of water and food and all rabbits were acclimatized for 1 month before handling in the experiments.

Experimental design. The 18 rabbits were divided into the following groups (Fig. 1). Control group (six rabbits for two time intervals): each rabbit received one dental implant on day 1 of the experiment. Three rabbits were sacrificed on day 30 of the experiment and the remaining three rabbits were sacrificed on day 45 of the experiment. Vitamin K₂ (six rabbits for two-time intervals): each rabbit received one dental implant on day 1 of the experiment with oral administration of vitamin K₂ once daily. Three rabbits were sacrificed on day 30 of the experiment and the remaining three rabbits were sacrificed on day 45 with continuous vitamin K₂ administration. Yerba mate extract (six rabbits for two-time intervals): each rabbit received one dental implant on day 1 of the experiment with oral administration of yerba mate extract once daily. Three rabbits were sacrificed on day 30 of the experiment and the remaining three rabbits were sacrificed on day 45 after continuous vitamin K₂ administration.

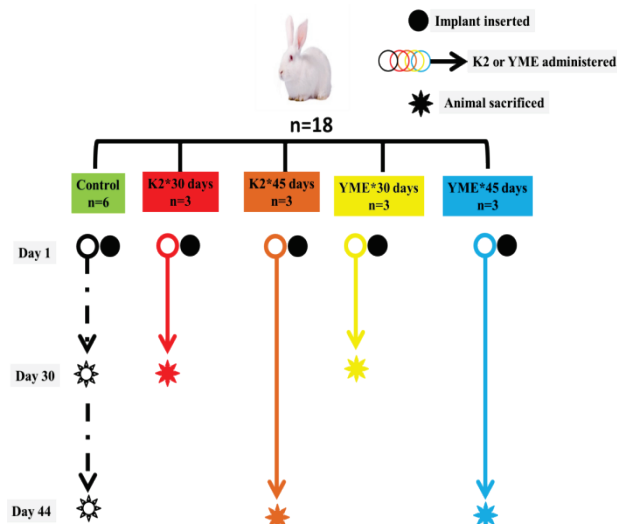


Fig. 1. Study design of the control and experimental rabbits used in the present research: YME – yerba mate extract, K₂ – vitamin K₂

Preparation and reconstitution of drugs: To prepare the yerba mate extract, 50 g of yerba mate was measured and combined with 300 mL of distilled water. This mixture was then heated on a heater at a temperature of 55 °C for 7 hours. After heating, the mixture was covered and allowed to rest overnight. The following day, the solution was filtered using filter paper to separate the liquid from the solid residue. The resulting liquid extract was air-dried, converting it into a powder form. Finally, the dried yerba mate powder was dissolved in distilled water and administered to the rabbit for the intended experimental application. Once prepared, 500 mg of the resulting powder was dissolved in water and administered orally to each rabbit each day. VK₂ capsules (Innerzyme, USA) were administered as 600 µg per rabbit per day after being reconstituted in a suitable volume of distilled water.

Surgical procedure of implantation. The rabbit fur around the proximal tibia was shaved and the skin surface was cleaned with iodine solution (povidone iodine) in the tibia metaphysis and left to dry before the surgery. Rabbits were anaesthetised with a combination of 10 mg/kg of ketamine hydrochloride (KetalromR, Romvac company, Romania) and 3 mg/kg of xylazine hydrochloride (XylaR, Intercheime, Holland) intramuscular. During surgery, all rabbits were infused with lactated Ringer's solution. After a 2 cm-incision was performed in the skin and subcutaneous tissues, the muscles and periosteum were dissected to expose the bone surface of the tibia metaphysis.

Starting with making a hole using the initial drill, 2.8-mm shaping drill, and 3.3-mm shaping drill, the implant fixture was inserted using each implant handpiece and torque ratchet (AnyOne fixture; internal type; diameter, 3.6 mm; length, 8.0 mm; Megagen, Daegu, Korea) (Hoffmann et al., 2012) (Fig. 2).



Fig. 2. Implant inserted in rabbit tibia

Samples with a diameter of 3.8 mm and length of 8 mm were thoroughly rinsed with sterile saline before insertion and positioned in the tibia metaphysis. The top part was cut and removed by a cutter to avoid tissue damage. The wound was closed with a resorbable 3.0 polyglycolic acid-coated white suture (Surgifit[®], Busan, Korea). Afterwards, the samples were allowed to be self-healed. The animals under surgery were given 1 mg/kg of Diclofenac sodium (OlfenR, Acino, Switzerland) and 10 mg/kg of Oxytetracyclin (LimoxinR, Ami Pharma, Jordan) were administered via intramuscular injection after surgery and 3 days after surgery, topical application of Gentamicin eye ointment (Genidin, Samara, Iraq) was administered in the wound area until it healed (Fig. 3).

To confirm proper surgical insertion of the implant on the tibial bone of the rabbit, the tibial bone site holding the implant was exposed to X-ray (Fig. 4).

To confirm the proper surgical insertion of the implant on the tibial bone of the rabbit, the tibial bone site holding the implant was removed from the sacrificed animal and the wool with skin was removed. The tissue was cleaned to expose the implant site (Fig. 5A). Moreover, the tissue built on the top of the implant was also removed to expose the implant (Fig. 5B, 5C). The implants were removed from the tissue insertion site (Fig. 5D) and the local tissue was collected for subsequent genetic, proteomic, and histological analysis.

Animal sacrifice and retrieval of specimen. The animals were killed, after 30 and 45 days of the experiment, via cervical spine dislocation once the experiment was finished. The tibia was dissected and a segment of metaphysis about 2.0 cm in length comprising the sample was obtained for histological study and gene extraction. All dissected bone segments were fixed in a 10% neutral-buffered formalin solution for 24 hours.

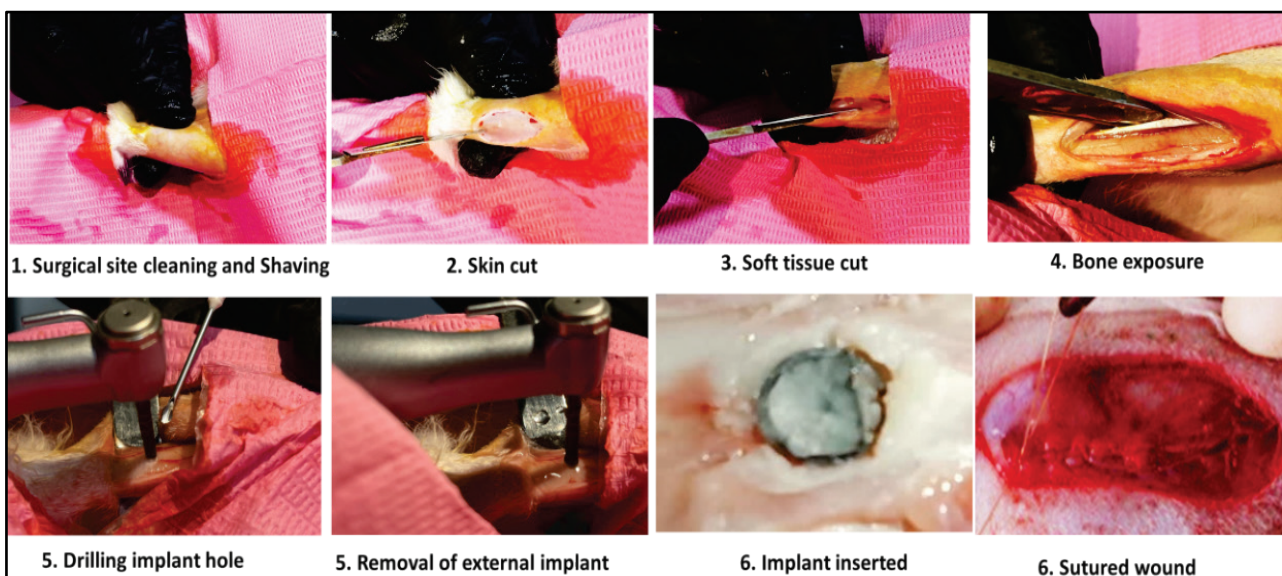


Fig. 3. Steps for implant insertion

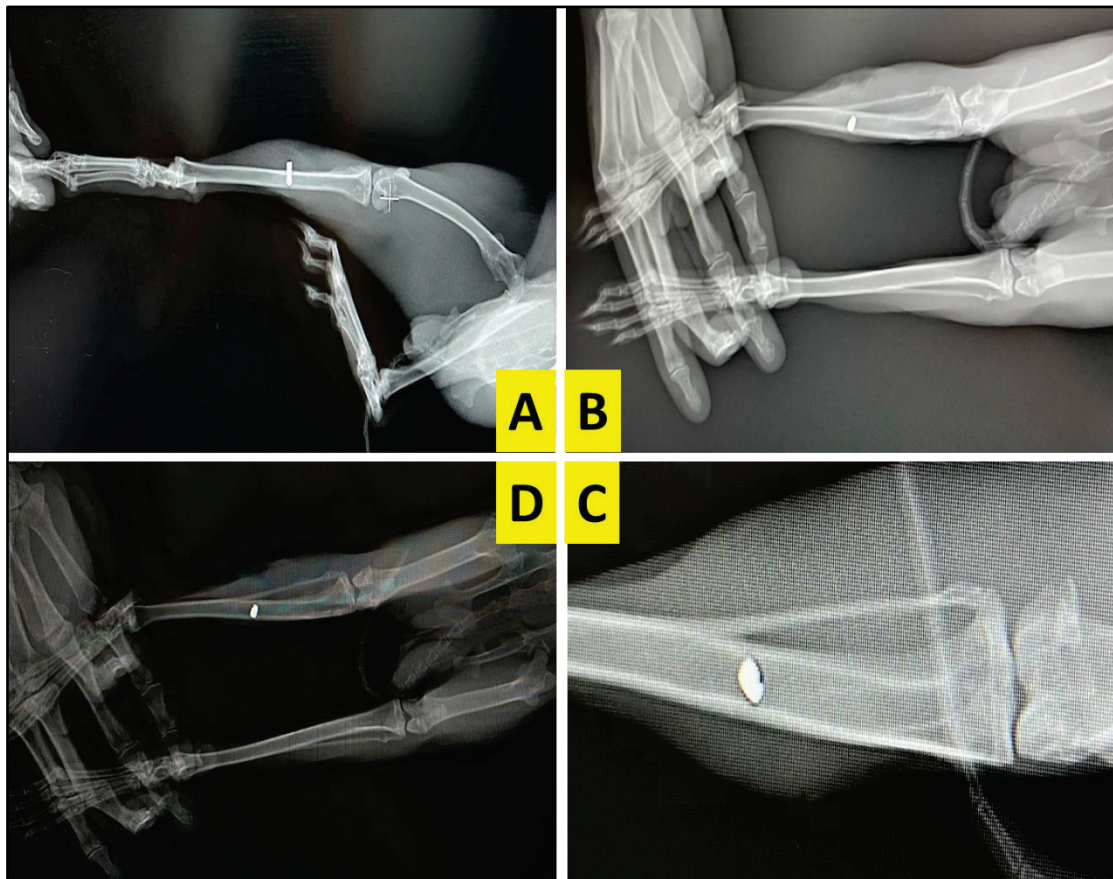


Fig. 4. Representative X-ray of the tibia bone with inserted implant localized inside the bone to confirm the proper surgical induction methods and well-maintained implant without failure: (A) side image, (B) anterior image, (C) close image, (D) top image

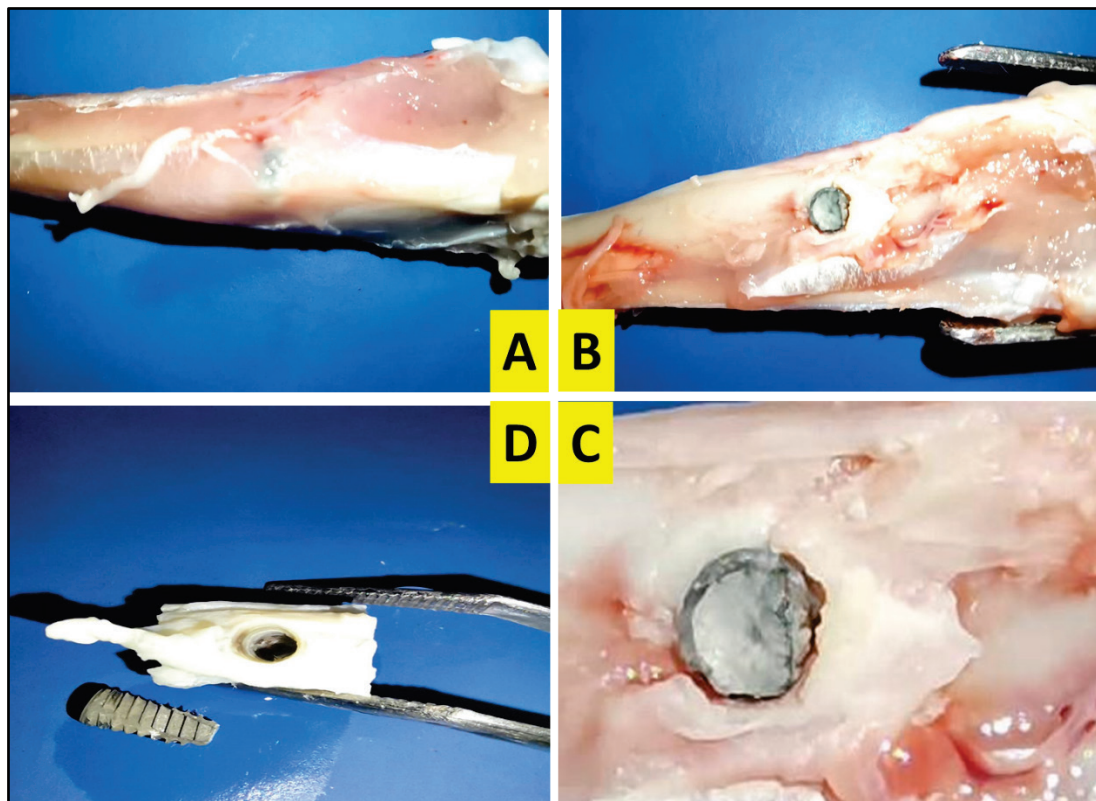


Fig. 5. Representative macroscopic picture (gross examination) of the tibia bone with inserted implant localized inside the bone to confirm the proper surgical induction methods and well-maintained implant without failure: (A) before removal of surrounding tissues around the implant, (B) after removal of the tissues around the implants, (C) clear image of the implant inside the bone before sampling, (D) collected tissues after implant removal

Histological preparation. After the samples were cleaned, they were dried with an ethanol gradient and then embedded in paraffin. Before the dehydration step, the tissue was decalcified in an EDTA-based decalcifying solution for five to seven days, depending on the tissue's structural density. Starting at the centre of the initial defect, the specimens were sliced into five-micrometer slices using a sliding microtome (Leica, Wetzlar, Germany) orientated transversely. After that, they were kept for the entire night in an oven set to 37 °C. After incubation, all slides were deparafinised with xylol, followed by rehydration with xylene for 10 minutes, then placed under running water for 5 minutes. Samples were stained with haematoxylin and eosin to identify areas of new bone formation.

$$\text{Percentage of newly formed bone (\%)} = \frac{\text{Newly formed bone area (mm}^2\text{)}}{\text{Newly formed bone area (mm}^2\text{)} + \text{Residual graft material (mm}^2\text{)} + \text{Connective tissue (mm}^2\text{)}}$$

Histopathological scoring was utilized to evaluate the repair of the bone defect in the following methods, based on predefined criteria. Furthermore, to evaluate the repair of the bone defect in the following methods, we adopted the following criteria: a score of 0 indicates neither the development of fibrous connective tissue nor bone. Grades 1 through 3 correspond to the following: full (>50%) and dense (>50%) bone formation and dense fibrous connective tissue formation, respectively; mild (<50%) and mild to moderate (>50%) bone formation and moderate to dense (>50%) fibrous connective tissue production, respectively.

Radiographic criteria. Radiographic assessment of the healing process of tibial bone defect was carried out, and a 70-cm focal film distance was used. Standard craniocaudal and lateromedial radiographs were obtained for each operated rabbit. All obtained radiographs were precisely interpreted until complete healing.

Blood sampling and serum separation. Following complete anaesthesia and before sacrificing the rabbit, the blood samples from control and intervention groups were taken from the heart using a 19–21 gauge needle, preferably the ventricle, which can be accessed either via the left side of the chest, through the diaphragm, from the top of the sternum or via a thoracotomy. Blood was withdrawn slowly to prevent the heart from collapsing. The serum samples were left to clot at ambient temperature for one hour, and centrifuged at 3000 rpm for 15 minutes and the separated serum samples were frozen down to –20 °C for further analysis.

Biochemical analysis criteria. Blood samples were taken from each group of animals and the separated serum was tested as per manufacturer instruction, for glutathione peroxidase (GSH-Px) (Catalog: FY-RA13532, Wuhan Feiyue Biotechnology, China), malondialdehyde (MDA), and total antioxidant capacity (Catalog No: FY-BC4517, Wuhan Feiyue Biotechnology, China).

RNA extraction and RT-PCR analysis. The initial stage in the PCR process was to isolate total RNA using a Promega RNA extraction kit in accordance with the manufacturer's instructions. The isolated RNA was then converted into cDNA using reverse transcriptase (RT). Priming was conducted at 25 °C for 10 minutes, reverse transcription at 50 °C for 60 minutes, RT inactivation at 80 °C for 5 minutes, and holding at 12 °C comprised the cycle technique. Using the Step-One Applied Biosystems tool system, USA, the final step of RT-PCR was carried out on cDNA samples pertaining to particular genes that were Osteocalcin: sense 5'-GAAGCCCAGCGGTGCA-3', antisense 5'-CAC TACCTCGCTGCCCTCC-3', Runx2: sense 5'-GCCT TCAAGGTGGTAGCCC-3', antisense 5'-CGTTACCGCCATGACAGTA-3' and housekeeping gene β -Actin sense 5'-GCGACCTCACCGACTACCT-3', antisense 5'-GCCATCTCGTTCTCGAA GTC-3'.

A final volume of 25 μ L was used for each reaction, which included 5.0 μ L of cDNA, 0.5 μ mol of sense and antisense specific primers for all primers 2.0 μ L, 5.5 μ L PCR water and 12.5 μ L of SYBER Green Supermix (BioRad, Hercules, CA, USA). A preincubation phase of 3 minutes at 95 °C was used to denaturise the template cDNA. This was followed by 40 cycles of denaturation (15 s at 95 °C), annealing (15 s at 60 °C), and extension (30 s at 72 °C) in the amplification procedure. Fluorescence was measured at 72 °C following each cycle. For every experiment, a negative control with no

Using a light microscope (Miotic, China), a skilled and blinded examiner carried out histological evaluations, including histomorphometry. A digital camera (AmiScope, China) was used to take high-resolution pictures. Using the associated 5 mm initial defect area as the region of interest, the AmiScope Standard Imaging Software (Version 2.1, China) performed the histomorphometric analysis. Both the initial defect area and the area of the newly produced bone were measured. Both newly formed bone and remaining transplant material were included in the total bone area (measured in millimetres squared). This formula, which has been applied in other studies, was used to determine the percentage of newly formed bone in the entire defect region:

cDNA template was conducted. Samples were processed twice. Using the standard reactions for each target and housekeeping gene, standard curves were made by plotting the Ct values (cycle threshold) against the log cDNA dilution. This allowed relative quantification to be performed after PCR. The values were expressed by allocating a value of 1 to the relative mRNA level of control implants. The 2^{- $\Delta\Delta$ Ct} technique was used to extract the data as Ct values and calculate the fold change.

Statistical analysis. The statistical software SPSS (SPSS v26.0 for Windows, IBM, Chicago, USA) was used for the analyses. To evaluate whether the distribution of the data was normal, the Shapiro-Wilk test was utilized. One-way ANOVA and post hoc Tukey testing were used for group comparisons on data with a normal distribution, while the Kruskal-Wallis test was used for groups whose distributions were not normal. Furthermore, the Mann-Whitney U test or the independent-samples t test were employed to assess differences between two distinct groups. The data were displayed as median (min-max) or mean \pm SD, depending on the distribution properties of the data. A statistically significant P-value was defined as less than 0.05. An adjusted P value for multiple comparisons was obtained using the Bonferroni adjustment test. By dividing the number of feasible comparisons (n = 6) between groups by the P-level of 0.05, the adjusted significance level was determined to be 0.008.

Results

The comparison of histological bone sections of the VK2 treated group versus the control group revealed that those rabbits treated with VK2 over 30 days showed change in cellular morphology and new bone growth, which is typically associated by the production of tiny capillaries and collagen-rich membrane structures, and this was noted in all of the rabbit groups that received interventional therapy. The early ossification zones, which were rich in living osteoprogenitor cells and extremely dense in collagen fiber groups, were visible in the VK2 30- and 44-day groups. There were ordered cell forms in the lacunae. Osteoprogenitor cells were seen within and around intramembranous bone production islets in the VK2 45-day group. Surprisingly, severe infiltration with high numbers of eosinophils and inflammatory cells was observed clearly in the new bone formation foci, while there was also a large number of fibrocytes around the new capillaries indicating bone remodeling. However, the control group showed normal bone matrix with abundant presence of osteocytes and standard infiltration with fibrocytes, suggesting a stable bone structure consistent with typical physiological conditions.

The comparison of bone histological sections of the YME treated versus the control group revealed that those rabbits treated with YME showed signs of new bone growth, which was usually accompanied by the formation of small capillaries and collagen-rich membrane structures. The YME 30- and 45-day groups showed signs of early ossification zones, which were highly packed in collagen fibre and rich with live osteoprogenitor cells. In the lacunae, there were organized cell formations. In both YME groups, osteoprogenitor cells, osteoblasts, and osteocytes were observed within and around the islets of intramembranous bone formation (Fig. 6).

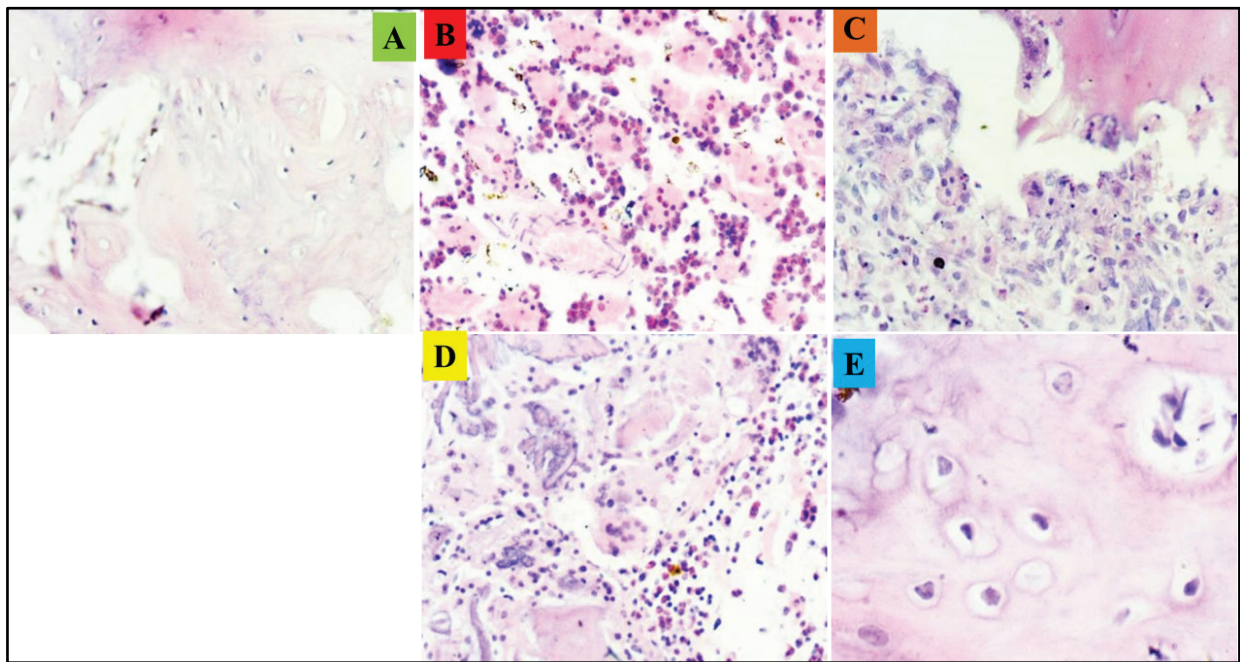


Fig. 6. A representative histological bone section from control rabbits and treated rabbits for 30 and 45 days: control sections showed a normal bone matrix with large numbers of osteocytes and normal infiltration with fibrocytes; treated sections revealed severe infiltration with eosinophils and other inflammatory cells, new tiny capillary formations, and collagen-rich membrane structures: (A) section from the control group, (B) section from VK2 after 30 days of treatment, (C) section from VK2 after 45 days treatment, (D) section from YME after 30 days treatment, (E) section from YME after 45 days treatment

The results of the quantitative analysis of new bone formation indicated that the percentage of newly formed bone in VK2 – 30-days group ($35.5 \pm 3.2\%$), VK2 – 45-days group ($43.2 \pm 2.1\%$), and YME-45-days group ($39.7 \pm 4.0\%$) were significantly ($P < 0.05$) higher than that of the control rabbits ($26.4 \pm 2.6\%$) group. However, the percentage of newly formed bone in the YME treated group ($27.4 \pm 6.3\%$) was non-significant ($P > 0.05$) compared to the control group. In comparison to the YME 45-day group, the VK2 45-day group displayed a considerably higher proportion of new bone production. Meanwhile, the VK2 30-day group also demonstrated a significant variation when compared to the YME 30-day group ($P < 0.05$, Fig. 7).

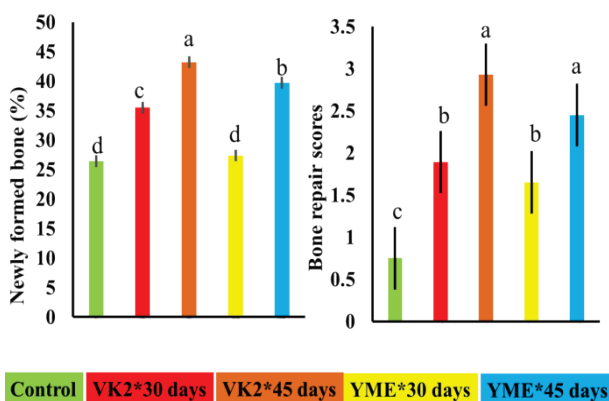


Fig. 7. Percentage of new bone formation tissue scale and bone repair scores in the investigated groups: YME and VK2 have improved bone formation compared to the control group ($P < 0.001$): data stated as mean \pm SD for each bar in the histogram; different letters express significant difference at $P < 0.05$ while the same letters express non-significant difference at using one-way ANOVA, the P differences in mean values were applied using Tukey's post hoc test; VK2 – vitamin K₂ and YME – yurba mate extract

In comparison to the control group (0.75 ± 0.21), all of the treated groups (the VK2 45-days group (2.93 ± 0.32), the VK2 30-days group (1.89 ± 0.15), YME 45-days group (2.45 ± 0.17), and YME 30-

days group (1.65 ± 0.40), showed significantly ($P < 0.05$) higher bone repair scores. The YME 45 days and VK2 45 days group had a significantly ($P < 0.05$) higher bone defect healing score compared to either group with 30 days treatment. However, there were no appreciable ($P > 0.05$) variations in the bone defect repair scores between the YME 30 days and VK2 30 days groups (Fig. 7).

The continuous administration of YME and VK2 to the rabbit groups for 30–44 days, led to a nearly one-fold decline ($P < 0.001$) in bone MDA (nmol/L) levels in all experimented groups of animals compared to the control group (20.5 ± 0.64), furthermore, YME had a more powerful influence on bone MDA than VK2 shown as decreasing values in the experimented rabbits ($P < 0.05$, Fig. 8).

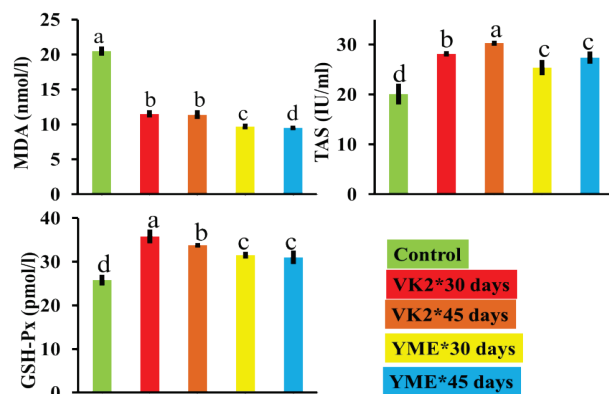


Fig. 8. Comparison of MDA, TAS, and GSH-Px levels in the investigated group: YME and vitamin K₂ have modulated the MDA levels compared to the control group ($P < 0.001$); data expressed stated as mean \pm SD for each bar in the histogram and the investigated groups are shown to be different statistically at $P < 0.05$ using one-way ANOVA, these differences in mean values were applied using Tukey's post hoc test; VK2 – vitamin K₂, YME – yurba mate extract, and MDA – malondialdehyde

The comparison of GSH-Px levels (pmol/L) of the VK2 or YME treated versus control group revealed that those rabbits treated over 30 or 44 days showed up to a 20–40% rise ($P = 0.002$) in bone GSH-Px

levels in contrast to the control group (25.8 ± 1.25). Moreover, the VK2 group showed higher bone concentration at day 30 or 44 post-treatment (35.8 ± 1.6 and 33.8 ± 0.52 , respectively) compared to YME post-treatment levels with parallel timepoints (31.5 ± 0.78 and 31.0 ± 1.55 , respectively, Fig. 8).

In comparison to the control group (20.1 ± 2.1), all of the treated groups [the VK2 30-days group (28.2 ± 0.54), VK2 45-days group (30.3 ± 0.5), YME 30-days group (25.4 ± 1.57), and YME 45-days group (27.4 ± 1.26)], showed significantly ($P < 0.05$) higher TAS levels. The VK2 30 days and VK2 45 days had significantly ($P < 0.05$) higher TAS compared YME groups. However, there were no appreciable ($P > 0.05$) variations in the TAS levels between YME 30 days and YME 45 days groups (Fig. 8).

The amplification curve of PCR that shows fluorescent unite cross cycles threshold (Ct value) was analyzed to compare the investigated groups. The bone Runx2 fold change jumped considerably in all treated groups [VK2 30-days (67.2 ± 0.5), VK2 45-days (66.5 ± 0.5), YME 30-days (52.2 ± 1.6), and YME 45-days (55.7 ± 1.3)] in comparison to the control group (41.6 ± 2.1). However, the fold of change was significantly higher in the VK2-treated groups compared to the treated group (Fig. 9).

The amplification curve of PCR that shows fluorescent unite cross cycles threshold (Ct value) was analyzed to compare the investigated groups. The bone osteocalcin fold change jumped considerably in all treated groups [VK2 30-days (27.14 ± 1.58), VK2 45-days (26.5 ± 0.53), YME 30-days (22.6 ± 0.78), and YME 45-days (25.5 ± 1.55)] in comparison to the control group (11.65 ± 1.25). However, the fold of change was significantly higher in both the VK2 treated groups and the YME 45-day treated group compared to the YME 30-day treated group (Fig. 9).

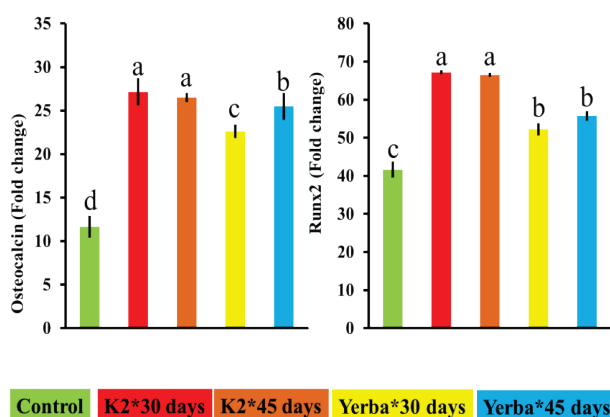


Fig. 9. Comparison of osteocalcin and Runx2 levels in the investigated group: YME and VK2 have modulated the osteocalcin levels compared to the control group ($P < 0.001$); data is stated as a fold of change for each bar in the histogram; different letters express significant differences at $P < 0.05$ while the same letters express non-significant differences using one-way ANOVA, these P differences in mean values were applied using Tukey's post hoc test; VK2 – vitamin K₂ and YME – yurba mate extract

Discussion

The findings of the present study confirmed that YME and VK2 had reasonable osseointegration impact of the implant on bone tissue in rabbit models, which could be harnessed for application in the treatment of bone disintegration due to different abnormalities or in dentistry. Moreover, YME and VK2 mitigated the oxidative stress associated with bone defects, facilitating and soothing the resolution step and hence improving the outcome of the injury.

The YME and VK2 had reduced oxidative stress indicated by elevated TAS and GSH-Px alongside reduced MDA with more intensive antioxidant effects shown with VK2. In line with the present study, previously published studies confirmed that VK tilts the balance of oxidative stress towards antioxidative effects through measuring the oxidant-antioxidant system in juvenile Jian carp which con-

firmed that *in vivo* antioxidant effects reciprocally correlated with the plasma VK levels (Yuan et al., 2016). Moreover, VK2 supplementation has potentially increased the expression of a promotor of multiple free radical scavenger pathways Nrf2 (nuclear factor erythroid-2-related factor 2) (El-Sherbiny et al., 2022; Lv et al., 2022). This pathway (Nrf2) is an intracellular protective mechanism that tackles oxidative stress by promoting the gene expression that is involved in the detoxification of free radicals (Mughtaridi et al., 2022). Bone implant surgery is associated with bone injury and hence oxidative stress leading to increased oxidative markers and this could interfere with bone healing and proper tissue regeneration (Hoffmann et al., 2012). Reducing oxidative markers as the case in the present study, using VK2, could potentially provide a tool for the treatment of bone injury.

Previous studies have been conducted and confirmed the antioxidant effects of YME and related these antioxidant effects to the presence of antioxidant vitamins and polyphenols (Matsumoto et al., 2009; Berté et al., 2014; Riachi & De Maria, 2017). Similarly, Pereira et al. (2017) reported that YME modulated oxidative stress markers, and this has been explained in the context of the presence of vitamins and polyphenolic compounds. Additionally, YME administration elevated blood glutathione in hyperlipidemic patients (Boaventura et al., 2012), and this impact has been related to the increased serum concentration of antioxidant biomolecules induced by YME (Lahouel et al., 2010), with the potential role of antioxidant vitamins in this antioxidant effect (Večeřa et al., 2003). Interestingly, one-week ingestion of YME has increased gene expression of GSH-Px (Matsumoto et al., 2009), elevated catalase activity (Berté et al., 2011), improved superoxide dismutase and reduced lipid peroxidation (Becker et al., 2019).

YME and VK2 have improved osseointegration of implants in the tibia bone of rabbits confirmed radiologically and histologically, which have shown proper integration of implants to the rabbit tibia alongside increased expression of osteogenic markers including osteocalcin and Runx2. In an *in vitro* study, YME has potentiated bone cell differentiation (Mukudai et al., 2014; Balera Brito et al., 2019), increased matrix protein deposition, potentiated alkaline phosphatase activity, and improved bone mineralization (Balera Brito et al., 2019) and confirmed by an *in vivo* study (Brasilino et al., 2018). In South America, the administration of YME to postmenopausal women has been associated with higher bone mineral density of the femoral head and lumbar spine (Conforti et al., 2012). Genetic markers including Runx2 and osteocalcin have shown improved expression in *in vitro* cell culture models when cells are exposed to YME (Kaback et al., 2008; Yuan et al., 2014).

VK has been tested for rat femoral osteotomy and the outcomes revealed that VK2 suppressed bone turnover and bone resorption while it stimulated lamellar bone formation, promoting bone healing and fracture repair (Iwamoto et al., 2010), these impacts have been explained in the context of anabolic effects of VK2 (Iwamoto et al., 2010). However, consistent clinical studies confirming the positive impacts of VK2 on osseointegration are lacking. In multi-centre studies it has been observed that VK is negatively associated with fracture risk (Cheung et al., 2008; Fusaro et al., 2012; Finnes et al., 2016; Moore et al., 2020). This outcome is not clear-cut because alternative interventional studies have shown discrepant outcomes, while some found a significant reduction in fracture risk (Huang et al., 2015; Maria et al., 2017; Mott et al., 2019), others did not (Tanaka et al., 2017; Su et al., 2019). The fracture rate was reduced in postmenopausal women and osteoporotic patients in a meta-analysis with a total of 11,112 participants by VK supplementation (Mott et al., 2019). This is contrasted with another meta-analysis study which showed no impact of VK in postmenopausal women (Su et al., 2019). The levels of OCN negatively correlated with SOS (speed of sound) with almost all showing low VK levels (Suzuki et al., 2017).

In a meta-analysis study involving 6,759 postmenopausal osteoporotic women, VK has provided potential improvement of vertebral BMD in osteoporotic women, but no response appeared in non-osteoporotic postmenopausal women (Huang et al., 2015), moreover, VK2 supplementation to healthy postmenopausal Danish women has shown negative impacts on BMD (Rønn et al., 2016). In alternative studies, a negative relationship between VK2 and BMD or osteoge-

nesis markers has been recorded (Tejero et al., 2016; Moore et al., 2020). The mechanism of VK2 in bone development is yet obscure, however, VK2 works as a coenzyme of Gla (γ -carboxyglutamic acid) proteins, which mediate mineralization (Hauschka et al., 1989), or a ligand for the SXR (steroid and xenobiotic receptor), which works as a support grid for bone via collagen assembly (Ichikawa et al., 2006).

Conclusion

The present study has confirmed that surface treatment with VK2 and YME has facilitated osseointegration and improved bone regeneration together with decreasing oxidative stress.

References

- Balera Brito, V. G., Chaves-Neto, A. H., Landim de Barros, T., & Penha Oliveira, S. H. (2019). Soluble yerba mate (*Ilex paraguariensis*) extract enhances *in vitro* osteoblastic differentiation of bone marrow-derived mesenchymal stromal cells. *Journal of Ethnopharmacology*, 244, 112131.
- Becker, A. M., Cunha, H. P., Lindenberg, A. C., de Andrade, F., de Carvalho, T., Boaventura, B. C. B., & da Silva, E. L. (2019). Spray-dried yerba mate extract capsules: Clinical evaluation and antioxidant potential in healthy individuals. *Plant Foods for Human Nutrition*, 74(4), 495–500.
- Berté, K. A., Beux, M. R., Spada, P. K., Salvador, M., & Hoffmann-Ribani, R. (2011). Chemical composition and antioxidant activity of yerba-mate (*Ilex paraguariensis* A.St-Hil., Aquifoliaceae) extract as obtained by spray drying. *Journal of Agricultural and Food Chemistry*, 59(10), 5523–5527.
- Berté, K., Rodríguez-Amaya, D. B., Hoffmann-Ribani, R., & Maccari Junior, A. (2014). Antioxidant activity of maté tea and effects of processing. In: Preedy, V. (Ed.). *Processing and impact on antioxidants in beverages*. Elsevier, Cambridge. Pp. 145–153.
- Brasilino, M. D. S., Stringheta-Garcia, C. T., Pereira, C. S., Pereira, A. A. F., Stringheta, K., Leopoldino, A. M., Crivelini, M. M., Ervolino, E., Dornelles, R. C. M., de Melo Stevanato Nakamune, A. C., & Chaves-Neto, A. H. (2018). Mate tea (*Ilex paraguariensis*) improves bone formation in the alveolar socket healing after tooth extraction in rats. *Clinical Oral Investigations*, 22(3), 1449–1461.
- Cheung, A. M., Tile, L., Lee, Y., Tomlinson, G., Hawker, G., Scher, J., Hu, H., Vieth, R., Thompson, L., Jamal, S., & Josse, R. (2008). Vitamin K supplementation in postmenopausal women with osteopenia (ECKO trial): A randomized controlled trial. *PLoS Medicine*, 5(10), e196.
- Conforti, A. S., Gallo, M. E., & Saraví, F. D. (2012). Yerba mate (*Ilex paraguariensis*) consumption is associated with higher bone mineral density in postmenopausal women. *Bone*, 50(1), 9–13.
- El-Sherbiny, M., Atef, H., Helal, G. M., Al-Serwi, R. H., Elkattawy, H. A., Shaker, G. A., Said, E., Abulfaraj, M., Albalawi, M. A., & Elsherbiny, N. M. (2022). Vitamin K₂ (MK-7) intercepts Keap-1/Nrf-2/HO-1 pathway and hinders inflammatory/apoptotic signaling and liver aging in naturally aging rat. *Antioxidants*, 11(11), 2150.
- Finnes, T. E., Lofthus, C. M., Meyer, H. E., Sogaard, A. J., Tell, G. S., Apalset, E. M., Gjesdal, C., Grimnes, G., Schei, B., Blomhoff, R., Samuelsen, S. O., & Holvik, K. (2016). A combination of low serum concentrations of vitamins K₁ and D is associated with increased risk of hip fractures in elderly Norwegians: a NOREPOS study. *Osteoporosis International*, 27(4), 1645–1652.
- Fusaro, M., Noale, M., Viola, V., Galli, F., Tripepi, G., Vajente, N., Plebani, M., Zaninotto, M., Guglielmi, G., Miotto, D., Dalle Carbonare, L., D'Angelo, A., Naso, A., Grimaldi, C., Miozzo, D., Giannini, S., Gallieni, M., & Vitamin K Italian (VIKI) Dialysis Study Investigators (2012). Vitamin K, vertebral fractures, vascular calcifications, and mortality: Vitamin K Italian (VIKI) dialysis study. *Journal of Bone and Mineral Research*, 27(11), 2271–2278.
- Hauschka, P. V., Lian, J. B., Cole, D. E., & Gundberg, C. M. (1989). Osteocalcin and matrix Gla protein: vitamin K-dependent proteins in bone. *Physiological Reviews*, 69(3), 990–1047.
- Hoffmann, O., Angelov, N., Zaffropoulos, G. G., & Andreana, S. (2012). Osseointegration of zirconia implants with different surface characteristics: An evaluation in rabbits. *The International Journal of Oral and Maxillofacial Implants*, 27(2), 352–358.
- Huang, Z. B., Wan, S. L., Lu, Y. J., Ning, L., Liu, C., & Fan, S. W. (2015). Does vitamin K₂ play a role in the prevention and treatment of osteoporosis for postmenopausal women: A meta-analysis of randomized controlled trials. *Osteoporosis International*, 26(3), 1175–1186.
- Ichikawa, T., Horie-Inoue, K., Ikeda, K., Blumberg, B., & Inoue, S. (2006). Steroid and xenobiotic receptor SXR mediates vitamin K₂-activated transcription of extracellular matrix-related genes and collagen accumulation in osteoblastic cells. *The Journal of Biological Chemistry*, 281(25), 16927–16934.
- Iwamoto, J., Seki, A., Sato, Y., Matsumoto, H., Tadeda, T., & Yeh, J. K. (2010). Vitamin K₂ promotes bone healing in a rat femoral osteotomy model with or without glucocorticoid treatment. *Calcified Tissue International*, 86(3), 234–241.
- Kaback, L. A., Soung, D. Y., Naik, A., Smith, N., Schwarz, E. M., O'Keefe, R. J., & Drissi, H. (2008). Osterix/Sp7 regulates mesenchymal stem cell mediated endochondral ossification. *Journal of Cellular Physiology*, 214(1), 173–182.
- Lv, J., Hou, B., Song, J., Xu, Y., & Xie, S. (2022). The relationship between ferroptosis and diseases. *Journal of Multidisciplinary Healthcare*, 15, 2261–2275.
- Maria, S., Swanson, M. H., Enderby, L. T., D'Amico, F., Enderby, B., Samsornaj, R. M., Dudakovic, A., van Wijnen, A. J., & Witt-Enderby, P. A. (2017). Melatonin-micronutrients osteopenia treatment study (MOTS): A translational study assessing melatonin, strontium (citrate), vitamin D₃ and vitamin K₂ (MK7) on bone density, bone marker turnover and health related quality of life in postmenopausal osteopenic women following a one-year double-blind RCT and on osteoblast-osteoclast co-cultures. *Aging*, 9(1), 256–285.
- Matsumoto, R. L., Bastos, D. H., Mendonça, S., Nunes, V. S., Bartchewsky, W., Ribeiro, M. L., & de Oliveira Carvalho, P. (2009). Effects of mate tea (*Ilex paraguariensis*) ingestion on mRNA expression of antioxidant enzymes, lipid peroxidation, and total antioxidant status in healthy young women. *Journal of Agricultural and Food Chemistry*, 57(5), 1775–1780.
- Moore, A. E., Kim, E., Dulnoan, D., Dolan, A. L., Voong, K., Ahmad, I., Gorska, R., Harrington, D. J., & Hampson, G. (2020). Serum vitamin K₁ (phylloquinone) is associated with fracture risk and hip strength in postmenopausal osteoporosis: A cross-sectional study. *Bone*, 141, 115630.
- Mott, A., Bradley, T., Wright, K., Cockayne, E. S., Shearer, M. J., Adamson, J., Lanham-New, S. A., & Torgerson, D. J. (2019). Effect of vitamin K on bone mineral density and fractures in adults: an updated systematic review and meta-analysis of randomised controlled trials. *Osteoporosis International*, 30(8), 1543–1559.
- Muchtaridi, M., Amirah, S. R., Harmonis, J. A., & Ikram, E. H. K. (2022). Role of nuclear factor erythroid 2 (Nrf2) in the recovery of long COVID-19 using natural antioxidants: A systematic review. *Antioxidants*, 11(8), 1551.
- Mukudai, Y., Kondo, S., Koyama, T., Li, C., Banka, S., Kogure, A., Yazawa, K., & Shintani, S. (2014). Potential anti-osteoporotic effects of herbal extracts on osteoclasts, osteoblasts and chondrocytes *in vitro*. *BMC Complementary and Alternative Medicine*, 14, 29.
- Riachi, L. G., & De Maria, C. A. B. (2017). Yerba mate: An overview of physiological effects in humans. *Journal of Functional Foods*, 38, 308–320.
- Rønn, S. H., Harsløf, T., Pedersen, S. B., & Langdahl, B. L. (2016). Vitamin K₂ (menaquinone-7) prevents age-related deterioration of trabecular bone microarchitecture at the tibia in postmenopausal women. *European Journal of Endocrinology*, 175(6), 541–549.
- Su, S., He, N., Men, P., Song, C., & Zhai, S. (2019). The efficacy and safety of menatetrenone in the management of osteoporosis: A systematic review and meta-analysis of randomized controlled trials. *Osteoporosis International*, 30(6), 1175–1186.
- Suzuki, Y., Maruyama-Nagao, A., Sakuraba, K., & Kawai, S. (2017). Level of serum undercarboxylated osteocalcin correlates with bone quality assessed by calcaneal quantitative ultrasound sonometry in young Japanese females. *Experimental and Therapeutic Medicine*, 13(5), 1937–1943.
- Tanaka, S., Miyazaki, T., Uemura, Y., Miyakawa, N., Gorai, I., Nakamura, T., Fukunaga, M., Ohashi, Y., Ohta, H., Mori, S., Hagino, H., Hosoi, T., Sugimoto, T., Itoi, E., Orimo, H., & Shiraki, M. (2017). Comparison of concurrent treatment with vitamin K₂ and risedronate compared with treatment with risedronate alone in patients with osteoporosis: Japanese Osteoporosis Intervention Trial-03. *Journal of Bone and Mineral Metabolism*, 35(4), 385–395.
- Tejero, S., Cejudo, P., Quintana-Gallego, E., Sañudo, B., & Oliva-Pascual-Vaca, A. (2016). The role of daily physical activity and nutritional status on bone turnover in cystic fibrosis: A cross-sectional study. *Brazilian Journal of Physical Therapy*, 20(3), 206–212.
- Yuan, J., Feng, L., Jiang, W.-D., Liu, Y., Jiang, J., Li, S.-H., Kuang, S.-Y., Tang, L., & Zhou, X.-Q. (2016). Effects of dietary vitamin K levels on growth performance, enzyme activities and antioxidant status in the hepatopancreas and intestine of juvenile Jian carp (*Cyprinus carpio* var. Jian). *Aquaculture Nutrition*, 22(2), 352–366.
- Yuan, Q., Jiang, Y., Zhao, X., Sato, T., Densmore, M., Schüler, C., Erben, R. G., McKee, M. D., & Lanske, B. (2014). Increased osteopontin contributes to inhibition of bone mineralization in FGF23-deficient mice. *Journal of Bone and Mineral Research*, 29(3), 693–704.